MATHEMATICAL BIOSCIENCES
AND ENGINEERING
Volume **13**, Number **2**, April **2016**

doi:10.3934/mbe.2015003

pp. **281–301**

ELECTRICAL-THERMAL ANALYTICAL MODELING OF MONOPOLAR RF THERMAL ABLATION OF BIOLOGICAL TISSUES: DETERMINING THE CIRCUMSTANCES UNDER WHICH TISSUE TEMPERATURE REACHES A STEADY STATE

J. A. López Molina and M. J. Rivera

Applied Mathematics Department, Universitat Politècnica de València
Camino de Vera 46022 Valencia, Spain

E. Berjano*

Biomedical Synergy, Electronic Engineering Department
Universitat Politècnica de València
Camino de Vera 46022 Valencia, Spain

(Communicated by Yang Kuang)

Abstract. It has been suggested that during RF thermal ablation of biological tissue the thermal lesion could reach an equilibrium size after 1-2 minutes. Our objective was to determine under which circumstances of electrode geometry (needle-like vs. ball-tip), electrode type (dry vs. cooled) and blood perfusion the temperature will reach a steady state at any point in the tissue. We solved the bioheat equation analytically both in cylindrical and spherical coordinates and the resultant limit temperatures were compared. Our results demonstrate mathematically that tissue temperature reaches a steady value in all cases except for cylindrical coordinates without the blood perfusion term, both for dry and cooled electrodes, where temperature increases infinitely. This result is only true when the boundary condition far from the active electrode is considered to be at infinitum. In contrast, when a finite and sufficiently large domain is considered, temperature reaches always a steady state.

1. **Introduction.** Monopolar radiofrequency (RF) thermal ablation of biological tissues is a high-temperature ablative technique which raises the tissue temperature over 50°C with the aim of irreversibly destroying the target tissue. The target tissue is localized around the active electrode, which has a very small area compared to the dispersive electrode, placed far from the target. Indeed, this procedure can be considered as a specific type of monopolar electrosurgical procedure in which there is good contact between active electrode and tissue, which implies a relatively

2010 *Mathematics Subject Classification.* Primary: 92C50, 35K05; Secondary: 35K99.

Key words and phrases. Analytical model, bioheat equation, blood perfusion, cooled electrode, cylindrical model, thermal ablation, radiofrequency ablation, spherical model, theoretical modeling.

Financial support: This work received financial support from the Spanish "Plan Estatal de Investigación, Desarrollo e Innovación Orientada a los Retos de la Sociedad" under Grant TEC2014−52383−C3−R (TEC2014−52383−C3−1−R).

*Corresponding author.

low value of impedance, and where voltage and current have low and high values respectively compared to other electrosurgical variants such as electrosurgical cutting.

RF thermal ablation is currently used for instance in RF ablation of tumors [1], pain therapy [2] and to eliminate cardiac arrhythmias [3]. To conduct monopolar RF thermal ablation, different designs of electrodes have been clinically used. Needle-like electrodes (see Fig. 1B) are employed in several medical fields such as tumor ablation [1], cardiac ablation [3], or dermatology [4], while electrodes with spherical geometry, such as ball-tip electrodes, are used in general surgery (Fig. 1A). In brief, two principal geometries are found in active electrodes for RF thermal ablation: spherical and cylindrical.

While dry RF electrodes are based on a simple piece of solid metal, others are internally cooled by circulating liquid (cooled electrodes). The idea behind this feature is to minimize overheating at the electrode-tissue surface and hence avoid heated tissue sticking to the electrode surface, and to maximize the thermal lesion by avoiding dehydration of the surrounding tissue. In general, cooled electrodes create larger lesions than dry electrodes [5]. Active electrodes with spherical or cylindrical geometries can hence be implemented as dry or cooled electrodes.

It has been suggested that the thermal lesion (e.g. assessed by 50°C isotherm) could grow with time during RF thermal ablation, and approaches an equilibrium size after 1-2 minutes [2]. Our objective was to determine the circumstances of electrode geometry (needle-like vs. ball-tip) and electrode type (dry vs. cooled) under which the temperature will reach a steady-state at any point in the tissue. Furthermore, since blood perfusion can be an important heat removal mechanism during RF heating [6], and could delay or even impede the steady-state, we also studied the effect of blood perfusion.

In order to study the thermal performance of RF thermal ablation in a cheaply and quickly theoretical modeling has been broadly used, employing both numerical and analytical methods [7]. Although numerical methods have produced highly realistic models, little effort has been made to search for analytical solutions. It has been pointed out that knowledge of the analytical solution for RF heating of biological tissues is important, since it involves a thorough understanding of the mathematical feature behind the physical phenomenon [8]. Analytical solutions can also be used to validate numerical solutions, since they provide an exact solution [9]. The singularity of current density, and hence the temperature around the electrodes, can only be understood by analytical solutions. For instance, Wiley and Webster [10] analyzed the current density distribution in the tissue under circular dispersive electrodes and found divergence of density current at the electrode edge, while previous numerical calculations by Overmyer et al [11] found a finite maximum at the same point. Analytical models of thermal performance of active electrodes are also difficult to find. Honig [12] conducted analytical calculations to estimate the power density and heat rise around active electrodes, with the aim of explaining the mechanism of electrosurgical cutting. Later, Erez and Shizter [13] used a one-dimensional analytical model in spherical coordinates to study the effect of different factors on the temperature distribution during RF thermal ablation. Haines and Watson [14] also proposed an analytical one-dimensional model to study the performance of a spherical electrode for RF cardiac ablation, which despite its simplicity, gave valuable insight into the mechanism of RF ablation. All these analytical models assumed numerous simplifications, such as the homogeneity

and isotropy of the tissue, blood perfusion rate unaffected by the heating process, no boiling of tissue during heating, and so on, which are considered in most current numerical models. More recently, Haemmerich et al [15] solved analytically the steady-state thermal problem for a needle-like cooled electrode for RF hepatic ablation. Our group has previously developed transient-time analytical models for RF thermal ablation including spherical [16] and cylindrical geometries [17].

In this study we have built one-dimensional analytical models of RF thermal ablation for two electrode geometries (spherical and cylindrical), two kinds of electrodes (dry and cooled), and two blood perfusion conditions (with and without including the blood perfusion term in the bioheat equation). The transit-time thermal problem was solved and the corresponding limit temperature was computed.

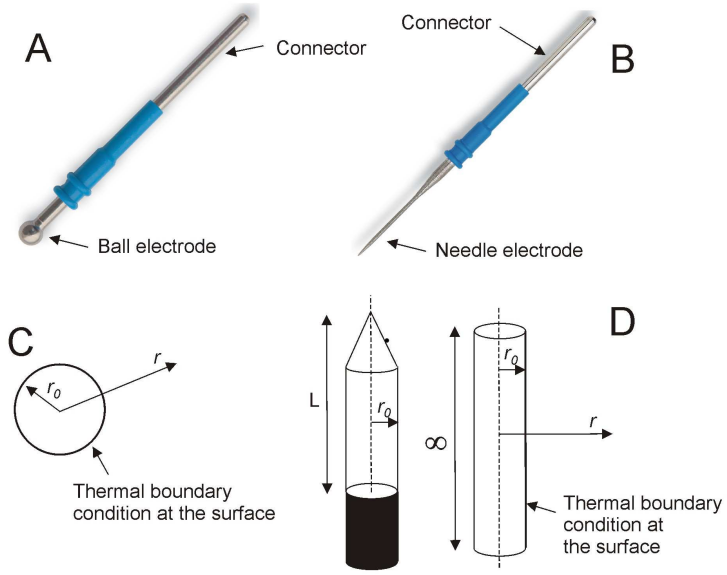

FIGURE 1. The most commonly employed geometries of active electrodes for RF thermal ablation: Ball tip (A) and needle tip (B) electrodes. C: Analytical model representing a simplified scenario with an ideal spherical metallic electrode of r_0 radius totally surrounded by homogeneous biological tissue. D: Analytical model representing a simplified scenario with an ideal cylindrical metallic electrode of r_0 radius and infinite length totally surrounded by homogeneous biological tissue. Both theoretical models (C and D) have one dimension, i.e. axis r. In the case of a cooled electrode, the internal cooling is modeled by means of a Dirichlet thermal boundary condition, in particular with a constant temperature (T_C), which corresponds to the temperature of the coolant flowing inside the electrode.

2. **Methods.** The general bioheat equation for RF thermal ablation is [7]

$$\eta\, c\, \frac{\partial T}{\partial t} = \nabla(k\, \nabla T) + S - \eta_b\, c_b\, \omega_b (T - T_b), \tag{1}$$

where T is the tissue temperature (°C), t is the time (s), η (kg/m^3); c $(\frac{J}{kgK})$ and k $(\frac{W}{m^2K})$ are the density, specific heat and thermal conductivity of the tissue respectively, η_b, c_b and ω_b $(1/s)$ are the density, specific heat and perfusion coefficient of the blood respectively, T_b is the blood temperature (°C) and S (W/m^3) represents the heat sources.

2.1. **Spherical geometry for ball-tip electrode modeling.** We considered a model geometry equal to those proposed by Erez and Shitzer [13], with a spherical electrode of radius r_0 completely embedded and in close contact with the biological tissue, which has an infinite dimension (Fig. 1C). As the model presented a radial symmetry a one-dimensional approach was possible.

Assuming all quantities η, η_b, c, c_b, k and ω_b of (1) to be constant and that the heat source is independent on the polar angle θ and working in spherical coordinates (r, θ), the equation (1) becomes

$$\eta\ c\ \frac{\partial T}{\partial t}(r,t) = k\left(\frac{\partial^2 T}{\partial r^2}(r,t) + \frac{2}{r}\frac{\partial T}{\partial r}(r,t)\right) + S(r,t) - \eta_b\ c_b\ \omega_b(T(r,t) - T_b). \quad (2)$$

Obviously $\omega_b = 0$ in the case of non perfusion.

Regarding the electrical problem, the source term for the RF heating modeling, i.e. the Joule heat produced per unit volume of tissue can be expressed as [13]:

$$S(r) = \frac{P\ r_0}{4\ \pi\ r^4},$$

where P is the total applied power (W), and r_0 the electrode radius (m). The resulting equation in spherical coordinates is

$$-\left(\frac{\partial^2 T}{\partial r^2}(r,t) + \frac{2}{r}\ \frac{\partial T}{\partial r}(r,t)\right) + \frac{\eta c}{k}\frac{\partial T}{\partial t}(r,t) = \frac{P\ r_0}{4\ \pi\ k\ r^4} - \frac{\eta_b c_b w_b}{k}(T - T_b), \quad (3)$$

T and r being temperature and dimension, respectively. The initial condition in the ball-tip electrode is

$$T(r,0) = T_0 \quad \forall\ r > r_0, \quad (4)$$

where T_0 is the initial temperature. The boundary condition far from the active electrode is assumed to be at infinitum (as done in previous modeling studies)

$$\lim_{r\to\infty} T(r,t) = T_0 \quad \forall\ t > 0. \quad (5)$$

In order to model the type of electrode (dry or cooled), we considered two different boundary condition in $r = r_0$. In the case of dry electrode, we adopted a simplification used in [13], which assumes the thermal conductivity of the electrode to be much greater than that of the tissue, i.e. assuming that the boundary condition at the interface between electrode and tissue is mainly governed by the thermal inertia of the electrode. At every time t the modulus of the heat flux along the surface electrode by unit time $\frac{\partial T}{\partial r}(r_0,t)$ is therefore inverted to produce a heat increment in the mass electrode equal to

$$\eta_0\ c_0\ \frac{4\ \pi r_0^3}{3}\frac{\partial T}{\partial t}(r_0,t),$$

where η_0 and c_0 are the density and specific heat of the active electrode, respectively. Then the boundary condition in $r = r_0$ is

$$4\ \pi\ k\ r_0^2\frac{\partial T}{\partial r}(r_0,t) = \eta_0\ c_0\ \frac{4\ \pi r_0^3}{3}\frac{\partial T}{\partial t}(r_0,t). \quad (6)$$

On the other hand, to model the cooled electrodes we assumed that the surface temperature is maintained at the coolant temperature, i. e. we used a Dirichlet boundary condition (DC)

$$T(r_0,t) = T_C \quad \forall\, t > 0, \tag{7}$$

where T_C is the coolant temperature. Although it has been previously suggested that theoretical modeling of RF thermal ablation with cooled electrodes should consider the modeling of a pre-cooling period along with a boundary condition based on Newton's cooling law rather than DC [18], this is only important for short periods of heating. Since we are now interested in the temperature at the infinitum time, using a DC can be a good approximation.

2.2. **Cylindrical geometry for needle-like electrode modeling.** By assuming all quantities η, η_b, c, c_b, k and ω_b to be constant, the heat source is independent of the polar angle θ, and working in cylindrical coordinates (r,θ), the equation (1) becomes:

$$\eta\, c\, \frac{\partial T}{\partial t}(r,t) = k\left(\frac{\partial^2 T}{\partial r^2}(r,t) + \frac{1}{r}\frac{\partial T}{\partial r}(r,t)\right) + S(r,t) - \eta_b\, c_b\, \omega_b(T(r,t) - T_b). \tag{8}$$

We employed the same formulation used by Haemmerich et al [15], and hence we have:

$$\eta\, c\, \frac{\partial T}{\partial t}(r,t) = k\left(\frac{\partial^2 T}{\partial r^2}(r,t) + \frac{1}{r}\frac{\partial T}{\partial r}(r,t)\right) + \frac{j_0^2\, r_0^2}{\sigma\, r^2} - \eta_b\, c_b\, \omega_b(T(r,t) - T_b), \tag{9}$$

where j_0 is the density current at the conductor surface (A/m^2) and σ is the electrical conductivity of tissue (S/m).

The problem to be solved is (9) with the conditions

$$T(r,0) = T_0 \quad \forall\, r > r_0 \tag{10}$$

$$\lim_{r\to\infty} T(r,t) = T_0 \quad \forall\, t > 0. \tag{11}$$

In order to model a cylindrical dry electrode, we assumed that the temperature flux along the surface of a small slice (dz) of electrode in an interval of time dt produced an amount of heating in the slice. Then

$$2\pi r_0 k \frac{\partial T}{\partial r}(r_0,t)\, dz = c_0\eta_0\pi r_0^2 \frac{\partial T}{\partial t}\, dz$$

and the boundary condition is hence

$$2k\frac{\partial T}{\partial r}(r_0,t) = c_0\eta_0 r_0 \frac{\partial T}{\partial t}(r_0,t) \quad \forall t > 0. \tag{12}$$

The cylindrical cooled electrode was modeled by using a DC as in equation (7).

2.3. **Dimensionless variables.** We shall use the following dimensionless variables:

$$\rho := \frac{r}{r_0}; \quad \xi := \frac{\alpha\, t}{r_0^2}; \quad \beta := \frac{\eta_b c_b w_b r_0^2}{k}; \quad V(\rho,\xi) := \kappa\, \left(T\Big(r_0\,\rho, \frac{r_0^2\,\xi}{\alpha}\Big) - T_0\right), \tag{13}$$

where α is the thermal diffusivity $(= \frac{k}{c\eta})$, $\kappa = \frac{4\,\pi\,k\,r_0}{P}$ in the case of spherical coordinates and $\kappa = \frac{\sigma k}{j_0^2 r_0^2}$ in the case of cylindrical coordinates.

Sometimes we will write $V(\rho,\xi,\beta)$ instead of $V(\rho,\xi)$ if we distinguish between case with perfusion ($\beta \neq 0$) and case without perfusion ($\beta = 0$). We denote by $V_H(\rho,\xi,\beta)$ the solution of the homogeneous problems associated to (3)

$$-\left(\frac{\partial^2 V_H}{\partial \rho^2}+\frac{2}{\rho}\frac{\partial V_H}{\partial \rho}\right)+\frac{\partial V_H}{\partial \xi}=-\beta\, V_H \tag{14}$$

and to (8)

$$-\left(\frac{\partial^2 V_H}{\partial \rho^2}+\frac{1}{\rho}\frac{\partial V_H}{\partial \rho}\right)+\frac{\partial V_H}{\partial \xi}=-\beta\, V_H. \tag{15}$$

We denote by $V_L(\rho,\beta)$ the dimensionless limit temperature, which is the limit $V_L(\rho,\beta) := \lim_{\xi\to\infty} V(\rho,\xi,\beta)$ as ξ approaches infinity. Although we are specially interested in obtaining the expression $V_L(\rho,\beta)$ for each considered case, we also consider the dimensionless steady state temperature, denoted by $V_{SS}(\rho,\beta)$, which corresponds to the solution of equations (3) and (8) when the partial derivative with respect to time is zero. Obtaining $V_{SS}(\rho,\beta)$ seems generally more straightforward than the $V_L(\rho,\beta)$ from the original problem (which includes the partial derivative with respect to time). The underlying question is whether $V_{SS}(\rho,\beta)$ is equal to $V_L(\rho,\beta)$.

2.4. **Tissue and electrode characteristics.** Once the limit temperature for each case was analytically obtained, we plotted it using Mathematica 6.0 software (Wolfram Research Inc., Champaign, IL, USA).Table I shows the characteristics of the elements used in the model. Blood temperature and the initial tissue temperature was $T_b = T_0 = 37°\text{C}$. The radius of all electrodes was considered to be $r_0 = 1.5\ mm$. A value of $T_C = 5°\text{C}$ was employed in the cases of cooled electrodes. In the case of cylindrical coordinates, a current density (j_0) of value 1.9 mA/mm^2 and 3.5 mA/mm^2 was used for dry and cooled electrodes, respectively, while in the case of spherical coordinates a total applied power of 1 W and 5 W was considered for dry and cooled electrodes, respectively. The applied power levels were chosen to avoid temperatures higher than 100°C in the tissue. Total applied power could not be estimated in the cylindrical case due to the infinite length of the modeled electrode. About the spherical electrode, higher power (5 W versus 1 W) was required in the case of the cooled electrode to obtain the same maximum temperatures as with the dry electrode. For the same reason, higher current density in the case of cylindrical electrode was required.

Table I. Thermal and electrical characteristics of the elements employed in the model [22], [23].

Element/Material	$\sigma(S/m)$	$k(\frac{W}{mK})$	$\eta(kg/m^3)$	$c(\frac{J}{kgK})$	$\omega(1/s)$
Electrode	-	-	21500	132	-
Tissue	0.33	0.502	1060	3600	-
Blood	-	-	1000	4148	$6.4\ 10^{-3}$

σ : electric conductivity; k : thermal conductivity; η : density; c : specific heat; ω : perfusion rate.

3. **Results.** The results section presents the analytical calculations conducted to obtain complete solutions of the dimensionless temperature for spherical and cylindrical geometries (Subsections 3.1 and 3.2, respectively). In each subsection, we first focused on the dry electrode (Subsections 3.1.1 and 3.2.1) and then on the cooled electrode (Subsections 3.1.2 and 3.2.2). Within each subsection, we first analyzed

the case with blood perfusion and then without. Finally, in Section 3.3., we assessed the impact of having assumed an electrode of infinite length in the cylindrical model and analyzed the consequences in terms of thermal performance.

3.1. **Temperature limit in spherical electrode.** The dimensionless equation for a spherical electrode is:

$$-\left(\frac{\partial^2 V}{\partial \rho^2}+\frac{2}{\rho}\frac{\partial V}{\partial \rho}\right)+\frac{\partial V}{\partial \xi}=\frac{1}{\rho^4}-\beta\, V. \tag{16}$$

It is straightforward that

$$V(\rho,\xi,\beta)=V_H(\rho,\xi,\beta)+V_{SS}(\rho,\beta),$$

$V_{SS}(\rho,\beta)$ being the steady state solution which satisfies the equation

$$-(V''_{SS}+\frac{2}{\rho}V'_{SS})=\frac{1}{\rho^4}-\beta V_{SS},$$

or equivalently

$$\rho^2 V''_{SS}+2\rho V'_{SS}-\beta\rho^2 V_{SS}=-\frac{1}{\rho^2}. \tag{17}$$

Let us suppose that for a specific set of initial and boundary conditions the steady state problem (17) has a solution. Due to the associated homogeneous problem (14) not having a heat source term, the limit temperature of $V_H(\rho,\xi,\beta)$ will be constant, and this constant must be zero, otherwise $V_{SS}(\rho,\beta)$ would not be the complete steady state temperature. In conclusion, if $V_{SS}(\rho,\beta)$ exists,

$$V_L(\rho,\beta)=V_{SS}(\rho,\beta).$$

Note that on many occasions it is easier to solve the steady state problem (17) and obtain $V_{SS}(\rho,\beta)$ than solve the original problem (3) and obtain $V_L(\rho,\beta)$ by using $V_L(\rho,\beta)=\lim_{\xi\to\infty} V(\rho,\xi,\beta)$.

3.1.1. *Temperature limit in dry spherical electrode.* The problem (3) becomes

$$-\left(\frac{\partial^2 V}{\partial \rho^2}+\frac{2}{\rho}\frac{\partial V}{\partial \rho}\right)+\frac{\partial V}{\partial \xi}=\frac{1}{\rho^4}-\beta\, V \tag{18}$$

with the dimensionless initial and boundary condition such that:

$$V(\rho,0)=0 \quad \forall\, \rho>1 \tag{19}$$

$$\lim_{\rho\to\infty} V(\rho,\xi)=0 \quad \forall\, \xi>0. \tag{20}$$

The dimensionless boundary condition for the dry electrode at the electrode surface is

$$\frac{m}{3}\frac{\partial V}{\partial \xi}(1,\xi)=\frac{\partial V}{\partial \rho}(1,\xi) \quad \forall\, \xi>0, \tag{21}$$

where $m=\frac{\eta_0\, c_0}{\eta\, c}$ is the dimensionless electrode thermal inertia.

The steady state equation is (17) with the boundary conditions $\lim_{\rho\to\infty} V_{SS}(\rho,\beta)=0 \quad \forall\, \xi>0$ and $V'_{SS}(1,\beta)=0$.

In the case without blood perfusion ($\beta=0$), the resolution of (17) is immediate

$$V_{SS}(\rho,0)=\frac{2\rho-1}{2\rho^2}.$$

This analytical solution allows to estimate the thermal lesion radius, assessed by means of the 50°C isotherm. The point r_{50} in which temperature attains 50°C can be expressed in function of the electrode radius r_0 and the applied power P as

$$r_{50} = \frac{P + \sqrt{P^2 - 104\ k\ \pi\ P\ r_0}}{104\ k\ \pi}.$$

In the case with blood perfusion ($\beta \neq 0$), first of all we have to solve the associate homogeneous equation

$$\rho^2 V''_{HSS} + 2\rho V'_{HSS} - \beta\rho^2 V_{HSS} = 0.$$

With the change of function $V_{HSS}(\rho) = \rho^{-1/2} U(\rho)$ we obtain the modified Bessel equation

$$\rho^2 U'' + \rho U' - (1/4 + \beta\rho^2) U = 0.$$

Then

$$\begin{aligned} U(\rho) =& A_1\ I_{\frac{1}{2}}(\sqrt{\beta}\rho) + A_2\ I_{-\frac{1}{2}}(\sqrt{\beta}\rho) \\ =& A_1 \left(\frac{2}{\pi\sqrt{\beta}\rho}\right)^{\frac{1}{2}} \sinh(\sqrt{\beta}\rho) + A_2 \left(\frac{2}{\pi\sqrt{\beta}\rho}\right)^{\frac{1}{2}} \cosh(\sqrt{\beta}\rho) \\ =& C_1 \frac{e^{\sqrt{\beta}\rho}}{\sqrt{\rho}} + C_2 \frac{e^{-\sqrt{\beta}\rho}}{\sqrt{\rho}}, \end{aligned} \tag{22}$$

where A_1, A_2, C_1 and C_2 are integration constants and $I_{\frac{1}{2}}$ and $I_{-\frac{1}{2}}$ are the modified Bessel functions of first kind and orders $\frac{1}{2}$ and $-\frac{1}{2}$ respectively.

Hence

$$V_{HSS}(\rho) = C_1 \frac{e^{\sqrt{\beta}\rho}}{\rho} + C_2 \frac{e^{-\sqrt{\beta}\rho}}{\rho}.$$

And using the constants variation method and the boundary conditions we obtain

$$\begin{aligned} V_{SS}(\rho,\beta) =& \frac{1}{2\ \rho\sqrt{\beta}} \Big[\int_\rho^\infty \frac{e^{-\sqrt{\beta}(u-\rho)}}{u^3} du \\ &+ \int_1^\rho \frac{e^{-\sqrt{\beta}(\rho-u)}}{u^3} du + \frac{\sqrt{\beta}-1}{\sqrt{\beta}+1} \int_1^\infty \frac{e^{-\sqrt{\beta}(u+\rho-2)}}{u^3} du \Big]. \end{aligned} \tag{23}$$

Then for every β,

$$V_L(\rho,\beta) = V_{SS}(\rho,\beta).$$

It should be noted that $\lim_{\beta\to 0} V_{SS}(\rho,\beta) = V_{SS}(\rho,0)$, which proves that $V_{SS}(\rho,\beta)$ is continuous with respect to to β in $\beta = 0$.

3.1.2. *Temperature limit in cooled spherical electrode.* In this case we combine the dimensionless equation (18) with the conditions (19) and (20). The dimensionless boundary condition on the electrode surface is now

$$V(1,\xi,\beta) = -B \quad \forall\ \xi > 0, \tag{24}$$

where $B = \frac{4\pi k r_0}{P}(T_0 - T_c)$.

The dimensionless steady state temperature also satisfies equation (17) but the boundary conditions are now $\lim_{\rho\to\infty} V_{SS}(\rho,\beta) = 0 \quad \forall\ \xi > 0$ and $V_{SS}(1,\beta) = -B$.

In the case without blood perfusion ($\beta = 0$) the resolution of the corresponding steady state equation is immediate

$$V_{SS}(\rho,0) = \frac{(1-2B)\rho - 1}{2\rho^2}.$$

In the case with blood perfusion ($\beta \neq 0$), we proceed as in the case of the dry spherical electrode and the solution of the equation is:

$$V_{SS}(\rho,\beta) = -\frac{Be^{\sqrt{\beta}(\rho-1)}}{\rho} + \frac{1}{2\,\rho\sqrt{\beta}}\Big[\int_{\rho}^{\infty} \frac{e^{-\sqrt{\beta}(u-\rho)}}{u^3}du + \int_{1}^{\rho} \frac{e^{-\sqrt{\beta}(\rho-u)}}{u^3}du - \int_{1}^{\infty} \frac{e^{-\sqrt{\beta}(u+\rho-2)}}{u^3}du\Big]. \tag{25}$$

Here also the limit temperature, with or without perfusion, is $V_L(\rho,\beta) = V_{SS}(\rho, \beta)$, and $V_{SS}(\rho,\beta)$ is continuous with respect to to β in $\beta = 0$.

In conclusion, the temperature distribution produced by RF thermal ablation with spherical electrode converges at any point of the tissue, regardless of the electrode type (dry versus cooled) and perfusion blood (with versus without). Figure 2 shows the limit temperature profiles for the four cases considered. Maximum temperature reached in the tissue (around 90°C) was located almost on the electrode surface in the case of the dry electrode, while it was 2-3 *mm* deeper in the case of the cooled electrode. Note that the inclusion of blood perfusion implies a decrease in the temperature values.

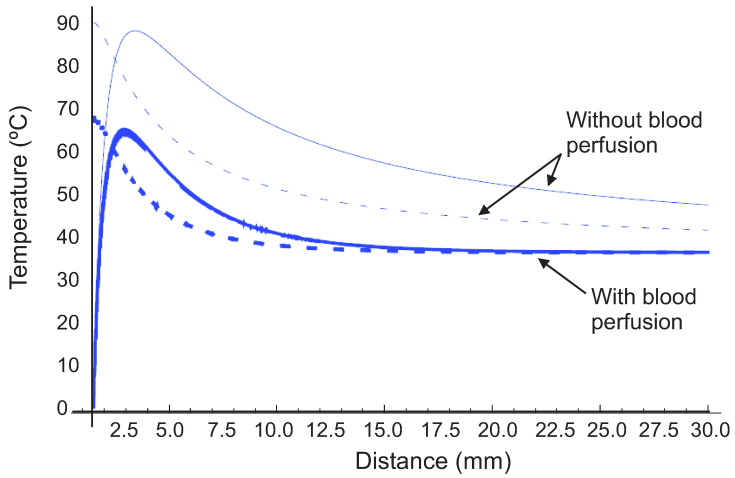

FIGURE 2. Limit temperature profiles computed for two types of spherical electrode: dry (dashed lines) and internally cooled (solid lines). For each type, two cases are considered: with and without the blood perfusion term included in the bioheat equation. The electrode radius was 1.5 *mm*, and the applied total power was 1 *W* and 5 *W* for dry and cooled electrodes, respectively. Coolant temperature was 5°C for the cooled electrode.

3.2. **Temperature limit in infinite cylindrical electrode.** The dimensionless equation for a cylindrical electrode is

$$-\left(\frac{\partial^2 V}{\partial \rho^2} + \frac{1}{\rho}\frac{\partial V}{\partial \rho}\right) + \frac{\partial V}{\partial \xi} + \beta V = \frac{1}{\rho^2}. \tag{26}$$

We also put

$$V(\rho,\xi,\beta) = V_{SS}(\rho,\beta) + V_H(\rho,\xi,\beta),$$

where the functions $V_{SS}(\rho,\beta)$ and $V_H(\rho,\xi,\beta)$ are the solutions of the steady state problem and the associated homogeneous problem respectively:

$$V''_{SS} + \frac{1}{\rho}V'_{SS} - \beta V_{SS} = -\frac{1}{\rho^2}, \tag{27}$$

$$-\left(\frac{\partial^2 V_H}{\partial\rho^2} + \frac{1}{\rho}\frac{\partial V_H}{\partial\rho}\right) + \frac{\partial V_H}{\partial\xi} + \beta V_H = 0. \tag{28}$$

As in the case of spherical electrode, if for determinate initial and boundary conditions the steady state problem has a solution, then

$$V_L(\rho,\beta) = V_{SS}(\rho,\beta).$$

3.2.1. *Temperature limit in infinite dry cylindrical electrodes.* The dimensionless equation for a dry cylindrical electrode is

$$-\left(\frac{\partial^2 V}{\partial\rho^2} + \frac{1}{\rho}\frac{\partial V}{\partial\rho}\right) + \frac{\partial V}{\partial\xi} + \beta V = \frac{1}{\rho^2} \tag{29}$$

$$V(\rho,0) = 0 \qquad \forall\rho > 1 \tag{30}$$

$$\lim_{\rho\to\infty} V(\rho,\xi) = 0 \quad \forall\,\xi > 0 \tag{31}$$

$$\frac{\partial V}{\partial\rho}(1,\xi) = \frac{m}{2}\frac{\partial V}{\partial\xi}(1,\xi) \quad \forall\xi > 0. \tag{32}$$

In the case with blood perfusion ($\beta \neq 0$), the equation of the steady state problem is the inhomogeneous modified Bessel equation

$$\rho^2 V''_{SS} + \rho V'_{SS} - \beta\rho^2 V_{SS} = -1, \tag{33}$$

whose solution, obtained by the method of variation of the parameters, is

$$\begin{aligned} V_{SS}(\rho,\beta) =& I_0(\sqrt{\beta}\rho)\left(-\int_1^\rho \frac{K_0(\sqrt{\beta}\,v)}{v}\,dv + M_1\right) \\ &+K_0(\sqrt{\beta}\,\rho)\left(\int_1^\rho \frac{I_0(\sqrt{\beta}\,v)}{v}\,dv + M_2\right), \end{aligned} \tag{34}$$

where I_0 and K_0 are the modified Bessel functions of order 0 of first and second kind, respectively and M_1, M_2 are constants to be selected to satisfy

$$\lim_{\rho\to\infty} V_{SS}(\rho) = 0 \tag{35}$$

$$V'_{SS}(1) = 0. \tag{36}$$

Then

$$M_1 = \int_1^\infty \frac{K_0(\sqrt{\beta}\,v)}{v}\,dv, \quad M_2 = \frac{I_1(\sqrt{\beta})}{K_1(\sqrt{\beta})}\int_\rho^\infty \frac{K_0(\sqrt{\beta}\,v)}{v}\,dv$$

and hence

$$\begin{aligned} V_L(\rho,\beta) =& V_{SS}(\rho,\beta) = I_0(\sqrt{\beta}\rho)\int_\rho^\infty \frac{K_0(\sqrt{\beta}\,v)}{v}\,dv \\ &+K_0(\sqrt{\beta}\rho)\left(\int_1^\rho \frac{I_0(\sqrt{\beta}\,v)}{v}\,dv + \frac{I_1(\sqrt{\beta})}{K_1(\sqrt{\beta})})\int_\rho^\infty \frac{K_0(\sqrt{\beta}\,v)}{v}\,dv\right). \end{aligned} \tag{37}$$

In the case without blood perfusion ($\beta = 0$), equation (33) becomes

$$V''_{SS} + \frac{1}{\rho} V'_{SS} = -\frac{1}{\rho^2} \tag{38}$$

which is an Euler's equation with general solution

$$V_{SS}(\rho) = C_1 + C_2 \log \rho - \frac{1}{2} \log^2 \rho,$$

with boundary conditions

$$\lim_{\rho \to \infty} V_{SS}(\rho) = 0 \tag{39}$$

$$V'_{SS}(1) = 0. \tag{40}$$

However it is impossible to satisfy the boundary condition at infinity (39) for every value of C_1 and C_2, which means that the steady state does not exist in this case. This gives us no information on the behavior of the limit temperature $V(\rho, \xi)$ when $\xi \to \infty$. We here need another approach, and this is provided by using the final value theorem of the Laplace transform.

Taking the Laplace transform $D(\rho, s, 0) := \mathfrak{L}[V](\rho, s, 0)$ in

$$-\left(\frac{\partial^2 V}{\partial \rho^2} + \frac{1}{\rho}\frac{\partial V}{\partial \rho}\right) + \frac{\partial V}{\partial \xi} = \frac{1}{\rho^2} \tag{41}$$

$$V(\rho, 0) = 0 \qquad \forall \rho > 1 \tag{42}$$

$$\lim_{\rho \to \infty} V(\rho, \xi) = 0 \quad \forall\, \xi > 0 \tag{43}$$

$$\frac{\partial V}{\partial \rho}(1, \xi) = \frac{m}{2}\frac{\partial V}{\partial \xi}(1, \xi) \quad \forall \xi > 0, \tag{44}$$

we obtain

$$\begin{aligned} D(\rho, s, 0) =& \frac{I_0(\rho\sqrt{s})}{s} \int_\rho^\infty \frac{K_0(v\sqrt{s})}{v}\, dv + \frac{K_0(\rho\sqrt{s})}{s} \int_1^\rho \frac{I_0(v\sqrt{s})}{v}\, dv \\ &+ K_0(\rho\sqrt{s}) \frac{\frac{2}{s}\sqrt{s} I_1(\sqrt{s}) - m I_0(\sqrt{s})}{m s K_0(\sqrt{s}) + 2\sqrt{s} K_1(\sqrt{s})} \int_1^\infty \frac{K_0(v\sqrt{s})}{v}\, dv, \end{aligned} \tag{45}$$

where I_1 and K_1 are the modified Bessel functions of order 1 of first and second kind respectively.

By the final value theorem of Laplace transform, the limit temperature will be

$$\begin{aligned} V_L(\rho, 0) &= \lim_{\xi \to \infty} V(\rho, \xi, 0) = \lim_{s \to 0} s\, D(\rho, s, 0) \\ &= \lim_{s \to \infty} [I_0(\rho\sqrt{s}) \int_1^\infty \frac{K_0(v\sqrt{s}}{v}\, dv - I_0(\rho\sqrt{s}) \int_1^\rho \frac{K_0(v\sqrt{s})}{v}\, dv \\ &+ K_0(\rho\sqrt{s}) \int_1^\rho \frac{I_0(v\sqrt{s})}{v}\, dv \\ &+ K_0(\rho\sqrt{s}) \frac{2\sqrt{s} I_1(\sqrt{s}) - m s I_0(\sqrt{s})}{m s K_0(\sqrt{s}) + 2\sqrt{s} K_1(\sqrt{s})} \int_1^\infty \frac{K_0(v\sqrt{s})}{v}\, dv] \\ &= \lim_{s \to 0} \left(I_0(\rho\sqrt{s}) + K_0(\rho\sqrt{s}) \frac{2\sqrt{s} I_1(\sqrt{s}) - m s I_0(\sqrt{s})}{m s K_0(\sqrt{s}) + 2\sqrt{s} K_1(\sqrt{s})} \right) \int_1^\infty \frac{K_0(v\sqrt{s})}{v}\, dv \\ &+ \lim_{s \to 0} \int_1^\rho \frac{K_0(\rho\sqrt{s}) I_0(v\sqrt{s}) - I_0(\rho\sqrt{s}) K_0(v\sqrt{s})}{v}\, dv. \end{aligned} \tag{46}$$

It is well known ([19]) that

$$K_0(z) = -I_0(z)\log\left(\frac{z}{2}\right) + Z(z) \tag{47}$$

where $Z(z)$ is an even holomorphic function on $\mathbb{C}$. We obtain

$$\begin{aligned}
&\lim_{s\to 0}\Big(K_0(\rho\sqrt{s})I_0(v\sqrt{s}) - I_0(\rho\sqrt{s})K_0(v\sqrt{s})\Big)\\
&\quad= \lim_{s\to 0} I_0(\rho\sqrt{s})I_0(v\sqrt{s})\Big(-\log\frac{\rho\sqrt{s}}{2} + \log\frac{v\sqrt{s}}{2}\Big)\\
&\quad= \lim_{s\to 0} I_0(\rho\sqrt{s})I_0(v\sqrt{s})\log\frac{v}{\rho} = \log\frac{v}{\rho}.
\end{aligned} \tag{48}$$

Then

$$\left|\lim_{s\to 0}\int_1^\rho \frac{K_0(\rho\sqrt{s})I_0(v\sqrt{s}) - I_0(\rho\sqrt{s})K_0(v\sqrt{s})}{v}\,dv\right| = \left|\int_1^\rho \log\frac{v}{\rho}\,\frac{dv}{v}\right| < \infty.$$

On the other hand, it is known that

$$K_1(z) = I_1(z)\log\frac{z}{2} + \frac{1}{z} + T(z), \tag{49}$$

where $T(z)$ is an odd holomorphic function on $\mathbb{C}$ ([19]) and by the L'Hôpital rule we obtain

$$\lim_{s\to 0}\sqrt{s}\log\frac{\rho\sqrt{s}}{2} = 0 \quad \text{and} \quad \lim_{s\to 0}\frac{\log\frac{\sqrt{s}}{2}}{\log\frac{\rho\sqrt{s}}{2}} = 1.$$

Then, by (47) and (49)

$$\begin{aligned}
&\lim_{s\to 0} K_0(\rho\sqrt{s})\frac{2\sqrt{s}I_1(\sqrt{s}) - msI_0(\sqrt{s})}{msK_0(\sqrt{s}) + 2\sqrt{s}K_1(\sqrt{s})}\\
&\quad= \lim_{s\to 0}\frac{\sqrt{s}\big(-I_0(\rho\sqrt{s})\log\frac{\rho\sqrt{s}}{2} + Z(\rho\sqrt{s})\big(2I_1(\sqrt{s}) - m\sqrt{s}I_0(\sqrt{s})\big)}{ms\big(-I_0(\sqrt{s})\log\frac{\sqrt{s}}{2} + Z(\sqrt{s})\big) + 2\sqrt{s}\big(I_1(\sqrt{s}\log\frac{\sqrt{s}}{2} + \frac{1}{\sqrt{s}} + T(\sqrt{s})\big)} = 0.
\end{aligned} \tag{50}$$

Finally, for every $M > 1$ we have

$$\lim_{s\to 0}\int_1^\infty \frac{K_0(v\sqrt{s})}{v}\,dv \geq \lim_{s\to 0}\int_1^M \frac{K_0(v\sqrt{s})}{v}\,dv \geq \lim_{s\to 0}\int_1^M \frac{K_0(M\sqrt{s})}{M}\,dv = \infty.$$

By putting together these results we obtain

$$\lim_{\xi\to\infty} V(\rho,\xi) = \lim_{s\to 0} s\; D(\rho,s,0) = \infty$$

which demonstrates that the temperature does not converge to a finite value when the time tends to infinity for every $\rho > 1$. If instead of the problem (29), (30), (31) and (32), (or the corresponding to the case bounded cylinder), we consider the same problem but changing condition (31) to the new condition $V(R,\xi) = 0$ for some fixed $R > r_0$, actually the new problem in the case without perfusion has the following solution

$$F(\rho,R) = \frac{1}{2}\Big(\log^2 R - \log^2\rho\Big).$$

In fact, $\lim_{R\to\infty} F(\rho,R) = \infty$. Although the steady state exists in the case with finite domain, the temperature values are huge compared to the case with perfusion (results not plotted).

3.2.2. *Temperature limit in infinite cooled cylindrical electrodes.* In the case of a cooled cylindrical electrode the steady state equation is again (33) and the solution (34), where M_1, M_2 are constants to be selected to satisfy

$$\lim_{\rho\to\infty} V_{SS}(\rho) = 0 \tag{51}$$

$$V_{SS}(1) = -B, \tag{52}$$

where now $B = \frac{\sigma k}{j_0^2 r_0^2}(T_0 - T_c)$.

In the case with blood perfusion ($\beta \neq 0$), we obtain

$$M_1 = \int_1^\infty \frac{K_0(\sqrt{\beta}\, v)}{v}\, dv, \quad M_2 = \frac{-1}{K_0(\sqrt{\beta})}\left(B + I_0(\sqrt{\beta}) \int_1^\infty \frac{K_0(\sqrt{\beta}\, v)}{v}\, dv\right).$$

Then in this case

$$\begin{aligned} V_L(\rho,\beta) = & V_{SS}(\rho,\beta) = I_0(\sqrt{\beta}\rho) \int_\rho^\infty \frac{K_0(\sqrt{\beta}\, v)}{v}\, dv + K_0(\sqrt{\beta}\rho) \int_1^\rho \frac{I_0(\sqrt{\beta} v)}{v}\, dv \\ & -B\frac{K_0(\sqrt{\beta}\rho)}{K_0(\sqrt{\beta})} - I_0(\sqrt{\beta})\frac{K_0(\sqrt{\beta}\rho)}{K_0(\sqrt{\beta})} \int_1^\infty \frac{K_0(\sqrt{\beta} v)}{v}\, dv. \end{aligned} \tag{53}$$

In the case without blood perfusion ($\beta = 0$), (34) also becomes

$$V''_{SS} + \frac{1}{\rho} V'_{SS} = -\frac{1}{\rho^2} \tag{54}$$

and then

$$V_{SS}(\rho) = C_1 + C_2 \log\rho - \frac{1}{2}\log^2\rho.$$

By adding the contour conditions,

$$\lim_{\rho\to\infty} V_{SS}(\rho) = 0 \tag{55}$$

$$V_{SS}(1) = -B \tag{56}$$

as in the case of the cylindrical dry electrode without perfusion we note that it is impossible to satisfy the boundary conditions at infinity, whatever the value of C_1 and C_2, which means that the steady state does not exist in this case.

After Laplace transformation $D(\rho, s, 0) := \mathfrak{L}[V](\rho, s, 0)$ in (29), (42), (43) and (24), we obtain

$$\rho^2 \frac{d^2 D}{d\rho^2} + \rho \frac{dD}{d\rho} - s\rho^2 D = -\frac{1}{s} \tag{57}$$

$$\lim_{\rho\to\infty} D(\rho, s, 0) = 0 \tag{58}$$

$$D(1, s, 0) = -\frac{B}{s}, \tag{59}$$

whose solution is

$$\begin{aligned} D(\rho,s,0) = & \frac{1}{s}\, I_0(\rho\sqrt{s}\,) \int_\rho^\infty \frac{K_0(v\sqrt{s}\,)}{v}\, dv + \frac{1}{s}\, K_0(\rho\sqrt{s}\,) \int_1^\rho \frac{I_0(v\sqrt{s}\,)}{v}\, dv \\ & -B\, \frac{K_0(\rho\sqrt{s}\,)}{s\, K_0(\sqrt{s}\,)} - I_0(\sqrt{s}\,)\, \frac{K_0(\rho\sqrt{s}\,)}{s\, K_0(\sqrt{s}\,)} \int_1^\infty \frac{K_0(v\sqrt{s}\,)}{v}\, dv. \end{aligned} \tag{60}$$

From equation (60) and by the final value theorem for Laplace transform we have

$$V_L(\rho, 0) = \lim_{\xi\to\infty} V(\rho, \xi) = \lim_{s\to 0} s\, D(\rho, s, 0).$$

To compute this limit we begin by defining

$$f(\rho, v, s) := \left(I_0(\rho\sqrt{s}) K_0(v\sqrt{s}) - I_0(\sqrt{s}) K_0(v\sqrt{s}) \frac{K_0(\rho\sqrt{s})}{K_0(\sqrt{s})} \right)$$

and hence

$$D(\rho, s, 0) = \int_\rho^\infty \frac{f(\rho, v, s)}{v\ s}\ dv - B\ \frac{K_0(\rho\sqrt{s})}{s\ K_0(\sqrt{s})} + \int_1^\rho \frac{f(v, \rho, s)}{v\ s}\ dv.$$

By (47) we have

$$\lim_{s\to 0} \frac{K_0(v\sqrt{s}\,)}{K_0(\sqrt{s}\,)} = \lim_{s\to 0} \frac{\log \frac{v\sqrt{s}}{2}}{\log \frac{\sqrt{s}}{2}} = 1 \tag{61}$$

and

$$\begin{aligned} \lim_{s\to 0} f(\rho, v, s) &= \lim_{s\to 0} \frac{K_0(v\sqrt{s}\,)}{K_0(\sqrt{s}\,)} \Big(I_0(\rho\sqrt{s}) K_0(\sqrt{s}\,) - I_0(\sqrt{s}\,) K_0(\rho\sqrt{s}\,) \Big) \\ &= \lim_{s\to 0} \Big(-I_0(\rho\sqrt{s}\,) I_0(\sqrt{s}\,) \log \frac{\sqrt{s}}{2} + I_0(\sqrt{s}\,) I_0(\rho\sqrt{s}\,) \log \frac{\rho\sqrt{s}}{2} \Big) \\ &= \lim_{s\to 0} I_0(\rho\sqrt{s}\,) I_0(\sqrt{s}\,) \log \frac{\frac{\rho\sqrt{s}}{2}}{\frac{\sqrt{s}}{2}} = \log \rho. \end{aligned} \tag{62}$$

Moreover, for every $\rho \geq 1, s > 0$ and $v \geq 1$ we have $f(\rho, v, s) \geq 0$ because $I_0(x)$ is strictly increasing and $K_0(x)$ is strictly decreasing. Then, by (62) we obtain

$$\begin{aligned} \forall\ s > 0,\ \forall M > \rho, \quad \lim_{s\to 0} s \int_\rho^\infty \frac{f(\rho, v, s)}{v\ s}\ dv &\geq \lim_{s\to 0} \int_\rho^M \frac{f(\rho, v, s)}{v}\ dv \\ &= \int_\rho^M \frac{\log \rho}{v}\ dv = \log \rho \log \frac{M}{\rho} \end{aligned} \tag{63}$$

and since $M > \rho$ is arbitrary we obtain

$$\lim_{s\to 0} s \int_\rho^\infty \frac{f(\rho, v, s)}{v\ s}\ dv = \infty$$

which demonstrates that temperature increases infinitely when the blood perfusion term is not considered.

On the other hand, by (62) $f(v, \rho, s)$ is a continuous function of s and v in $[1, \rho] \times [0, s_0]$ if $s_0 > 0$. Then

$$\lim_{s\to 0} s \int_1^\rho \frac{f(v, \rho, s)}{v\ s}\ dv = \lim_{s\to 0} \int_1^\rho \frac{\log v}{v}\ dv \leq \log^2 \rho.$$

Then by (61) we obtain $\lim_{s\to 0} D(\rho, s, 0) = \infty$ and hence $\lim_{\xi\to\infty} V(\rho, \xi) = \infty$ for every $\rho > 1$. Again this happens since we are using a boundary condition at infinitum.

In conclusion, the temperature distribution produced by RF thermal ablation with a cylindrical electrode only converges when blood perfusion is considered, otherwise temperature rises infinitely. Note that this result is only true when the boundary condition far from the active electrode is considered to be at infinitum. If a finite and sufficiently large domain is considered, temperature reaches a steady state. In fact

If instead of the problem (41), (42), (43) and (44), we consider the same problem but changing conditions (43) and (44) to the new conditions (55) for some fixed

$R > r_0$, and (56) actually the new problem in the case without perfusion has the following solution

$$G(\rho, R) = -B + B\frac{\log \rho}{\log R} - \frac{1}{2}\log^2 \rho + \frac{1}{2}\log R \log \rho.$$

In fact, $\lim_{R\to\infty} G(\rho, R) = \infty$.

In the case with blood perfusion a limit temperature profile can be obtained, regardless of electrode type (dry versus cooled). Figure 3 shows these limit temperature profiles for the case with blood perfusion. As with spherical electrodes, maximum temperature reached in the tissue (around 90°C) was located almost on the electrode surface in the case of a dry electrode, while it was around 5 mm deeper in the case of a cooled electrode.

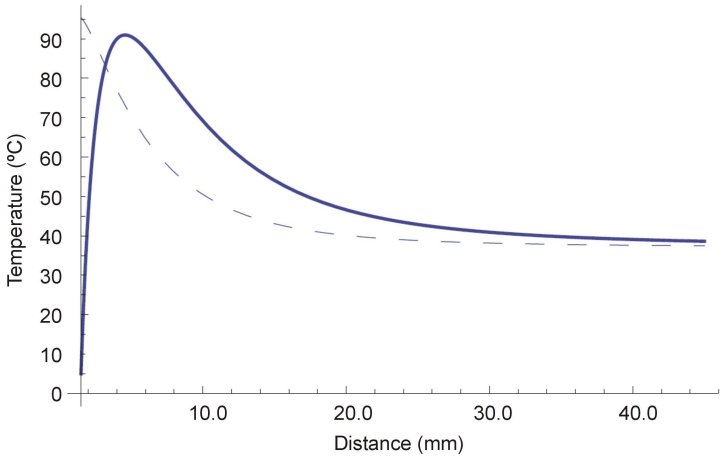

FIGURE 3. Limit temperature profiles computed for two types of cylindrical electrode: dry (dashed lines) and internally cooled (solid lines). The electrode radius was 1.5 mm, and the current density at the electrode surface (j_0) was 1.9 mA/mm^2 in the dry case and 3.5 mA/mm^2 in the cooled case. Coolant temperature was 5°C for the cooled electrode. Only the case with blood perfusion term is considered; the case without blood perfusion does not converge and hence no limit temperature can be computed.

3.2.3. *Temperature limit in a finite cylindrical electrode.* In Subsections 3.2.1 and 3.2.2, the cylindrical electrode was assumed to be infinitely long. This is really an important simplification and hence we had to check its impact on the conclusions. In this section we will demonstrate that this simplification is irrelevant from a qualitative point of view, i.e. in terms of how tissue temperature reaches the steady state. We solved a new problem by assuming a cylindrical electrode of length L. By assuming all quantities η, η_b, c, c_b, k and ω_b to be constant, the heat source is independent of the polar angle θ, and working in cylindrical coordinates (r, θ, z),

the formulation used by Haemmerich et al [15] of Equation (9) becomes:

$$\begin{aligned}\eta\, c\, \frac{\partial T}{\partial t}(r,z,t) =& k\left(\frac{\partial^2 T}{\partial r^2}(r,z,t)+\frac{1}{r}\frac{\partial T}{\partial r}(r,z,t)+\frac{\partial^2 T}{\partial z^2}(r,z,t)\right)\\ &+\frac{j_0^2\, r_0^2}{\sigma\, r^2}-\eta_b\, c_b\, \omega_b(T(r,z,t)-T_b)\end{aligned} \tag{64}$$

where j_0 is the density current at the conductor surface (A/m^2), σ is the electrical conductivity of tissue (S/m) and r_0 is the electrode radius (m). The problem to be solved is (64) with the conditions

$$T(r,z,0)=T_0 \quad \forall\, r>r_0, \quad z\in]0,L[\tag{65}$$

$$\lim_{r\to\infty} T(r,z,t)=T_0 \quad \forall\, t>0, \quad z\in]0,L[\tag{66}$$

$$2k\frac{\partial T}{\partial r}(r_0,z,t)=c\eta r_0\frac{\partial T}{\partial t}(r_0,z,t) \quad \forall t>0, \quad z\in]0,L[\tag{67}$$

and suitable boundary conditions in $z=0$ and $z=L$, for example an easy case could be $\frac{\partial T}{\partial z}(r,0,t)=\frac{\partial T}{\partial z}(r,L,t)=0$, $\forall r>r_0$, $\forall t>0$. We shall use the following dimensionless variables:

$$\rho:=\frac{r}{r_0}, w:=\frac{z}{L}, \xi:=\frac{\alpha\, t}{r_0^2}, \beta:=\frac{\eta_b c_b w_b r_0^2}{k}, \tag{68}$$

$$V(\rho,w,\xi):=\frac{4\,\pi\, k\, r_0}{P}\left(T\Big(r_0\,\rho, L\,w, \frac{r_0^2\,\xi}{\alpha}\Big)-T_0\right) \tag{69}$$

where α is the thermal diffusivity $(=\frac{k}{c\eta})$. Then the equation (64) becomes

$$-\left(\frac{\partial^2 V}{\partial\rho^2}+\frac{1}{\rho}\frac{\partial V}{\partial\rho}+D\frac{\partial^2 V}{\partial w^2}\right)+\frac{\partial V}{\partial\xi}=-\beta\, V+\frac{1}{\rho^2} \tag{70}$$

for some constant D, with

$$V(\rho,w,0)=0 \qquad \forall\rho>1, \quad 0<w<1 \tag{71}$$

$$\lim_{\rho\to\infty} V(\rho,w,\xi)=0 \quad \forall\,\xi>0, \quad 0<w<1 \tag{72}$$

$$\frac{\partial V}{\partial\rho}(1,w,\xi)=\frac{m}{2}\frac{\partial V}{\partial\xi}(1,w,\xi) \quad \forall\xi>0, \quad 0<w<1 \tag{73}$$

and the rest of boundary conditions in $w=0$ and $w=1$. The corresponding steady state problem is

$$-\left(\frac{\partial^2 V_{SS}}{\partial\rho^2}+\frac{1}{\rho}\frac{\partial V_{SS}}{\partial\rho}+D\frac{\partial^2 V_{SS}}{\partial w^2}\right)=-\beta\, V_{SS}+\frac{1}{\rho^2} \tag{74}$$

$$\lim_{\rho\to\infty} V_{SS}(\rho,w)=0 \quad 0<w<1 \tag{75}$$

$$\frac{\partial V_{SS}}{\partial\rho}(1,w)=0, \quad 0<w<1 \tag{76}$$

and the rest of boundary conditions in $w=0$ and $w=1$. We put $V_{SS}(\rho,w)=V_{SSH}(\rho,w)+F(\rho)$, where V_{SSH} satisfies the corresponding homogeneous equation

$$-\left(\frac{\partial^2 V_{SSH}}{\partial\rho^2}+\frac{1}{\rho}\frac{\partial V_{SSH}}{\partial\rho}+D\frac{\partial^2 V_{SSH}}{\partial w^2}\right)=-\beta\, V_{SSH} \tag{77}$$

and the corresponding boundary conditions, and $F(\rho)$ must satisfy

$$\rho^2 F''+\rho F'-\beta\rho^2 F=-1, \tag{78}$$

$$\lim_{\rho\to\infty} F(\rho)=0 \tag{79}$$

$$F'(1) = 0 \tag{80}$$

whose solution if $\beta \neq 0$ is

$$\begin{aligned} F(\rho) =& I_0(\sqrt{\beta}\rho) \int_\rho^\infty \frac{K_0(\sqrt{\beta}\, v)}{v}\, dv \\ &+ K_0(\sqrt{\beta}\rho) \left(\int_1^\rho \frac{I_0(\sqrt{\beta}\, v)}{v}\, dv + \frac{I_1(\sqrt{\beta})}{K_1(\sqrt{\beta})}) \int_1^\infty \frac{K_0(\sqrt{\beta}\, v)}{v}\, dv \right). \end{aligned} \tag{81}$$

Equation (77), with the corresponding boundary conditions, could be analytically solved by the separation of variables method. We suspect that it will not be a straightforward task for other boundary condition in $w = 0$ and $w = 1$. However, the conclusion is that the steady state temperature, and hence the final temperature, will also be finite in the case of a finite cylindrical electrode with blood perfusion. In contrast, in the case without blood perfusion ($\beta = 0$), Equation (78) becomes

$$F'' + \frac{1}{\rho} F' = -\frac{1}{\rho^2} \tag{82}$$

$$\lim_{\rho \to \infty} F(\rho) = 0 \tag{83}$$

$$F'(1) = 0. \tag{84}$$

The equation (82) is an Euler's equation with general solution

$$F(\rho) = C_1 + C_2 \log \rho - \frac{1}{2} \log^2 \rho.$$

But it cannot satisfy the boundary condition at infinity (83), for any values of C_1 and C_2, which means that the steady state does not exist in this case.

4. **Discussion.** The present study focused on the analytical study of the thermal performance at time infinity of the RF thermal ablation procedure. In particular, our objective was to determine under which circumstances of electrode geometry (spherical and cylindrical), electrode type (dry and cooled) and blood perfusion, the temperature reaches a steady-state at any point in the tissue. Knowing whether the temperature around the electrode during RF thermal ablation will reach a finite maximum value or whether it will rise indefinitely is crucial to understanding how thermal lesions are created in each case. In other words, whether the duration affects the lesion size or otherwise will be irrelevant from a certain time on.

Four analytical models of RF electrode were built and solved: dry spherical, cooled spherical, dry cylindrical and cooled cylindrical. For each electrode, we considered two cases: with and without a blood perfusion term in the bioheat equation. The case with blood perfusion could model the RF thermal ablation of a well perfused organ, such as liver or kidney, while the case without blood perfusion could model a procedure on a non perfused organ such as the cornea [20] or a well perfused organ on which a vascular clamping maneuver has been conducted during the heating. Although in all cases the transit-time thermal problem was addressed, a complete expression of the temperature over time was not obtained since we used the final value theorem for Laplace transform to compute the limit temperature in the cylindrical case without perfusion, i.e. the Laplace transforms were not inverted. As far as we know, this is the first analytical study which compares the thermal performance at time infinity of the most frequently used electrode geometries (spherical/cylindrical).

From a mathematical point of view, the most important finding was that tissue temperature reaches a steady value in all the cases studied, except for a cylindrical electrode in a tissue without blood perfusion, regardless of the electrode type (dry or cooled). The tendency towards overheating the tissue around the electrode is higher in cylindrical geometry than spherical. The reason is that while deposited power (W/m^3) decays at $1/r^2$ (current density at $1/r$) around cylindrical electrodes, around spherical electrodes it is faster, at $1/r^4$ (current density at $1/r^2$). This implies that power deposition is more circumscribed in the case of ball-tip electrodes compared with needle-like electrodes. This electrical performance leads to the temperature at any point always reaching a finite maximum value with spherical electrodes even in the case of tissue with blood perfusion. Conversely, the absence of the blood perfusion term in the case of cylindrical electrodes produces an infinite increase in the temperature, while the blood perfusion term is clearly the limiting factor in avoiding an uninterrupted temperature increase. Moreover, these conclusions are equally valid for both dry and cooled cylindrical electrodes, i.e. internal cooling is not a limiting factor in avoiding an uninterrupted temperature increase.

The conclusions about the cylindrical electrodes are only valid when the boundary condition far from the active electrode (i.e. where the dispersive electrode is placed) is considered to be at infinitum. In contrast, if we solve the same mathematical problem but considering a finite domain (although the boundary condition is enormously far), the temperature does not increase infinitely, and hence a steady state is reached in all cases. As a consequence, from a physical point of view, we can conclude that the tissue temperature reaches a steady state in all the cases studied.

Other minor findings (see plots in Figures 2 and 3) have already been reported in prior studies and can be summarized as: 1) the higher the blood perfusion rate, the lower the temperature value, 2) cooled electrodes produce a temperature peak shifted by a few millimeters within the tissue, whereas dry electrodes show a temperature peak located almost on the electrode surface, and 3) cooled electrodes produce lower values of maximal temperature than dry electrodes, but create larger lesions, as assessed by the 50°C isotherm.

4.1. **Limitations of the study.** The most important limitation of the analytical models developed in this study was that they did not include the dynamic changes in the tissue characteristics. The most important characteristic seems to be electrical conductivity (which does not appear explicitly in the equations of this study). Two dynamic changes in this characteristic are very important during an RF thermal ablation. The first occurs when tissue temperature begins to rise: electrical conductivity changes with temperature around $+2\%/°C$, which speeds up heating, as more RF power can be delivered to the tissue. The second change has to do with the desiccation associated with temperatures around 100°C. This phenomenon involves a large rise in impedance, which means the RF generator automatically stops controlling RF power delivery. This latter issue, which was not considered in our study, could also be an important factor in limiting the growth of the thermal lesion. In spite of this, our goal was also to demonstrate mathematically that even without including these dynamic changes, which could limit the rise in temperature, there exists a temperature limit profile in the majority of cases. In particular, the power density (W/m^3) decays very fast around a spherical electrode and this probably promotes the ability of the temperature to reach a stationary state. In contrast, the power density decays more slowly over the area around a cylindrical electrode, and this surely means thermal lesions are less constrained. Future numerical studies

should be conducted to check the validity of our conclusions when dynamic changes in tissue characteristics are included.

The models were one-dimensional, and hence in the case of cylindrical coordinates, they mimicked an electrode with infinite length placed in a tissue cylinder of infinite diameter. The needle-like electrodes actually have a sharp tip at the distal edge and a proximal edge which forms the interface between the metallic electrode and plastic cover. However, in a previous study, we demonstrated theoretically and experimentally that during the first seconds of heating with a needle-like cooled electrode the temperature at the distal and proximal edges quickly rises to 100°C [21], which implies that the tissue in these zones becomes almost dehydrated and hence the electrical current flows through the middle zone. This suggests that during the following seconds and minutes, the electrically active zone of the electrode is the middle zone, and hence the model based on a simple cylinder could be valid.

Our study considered a protocol of constant power for spherical electrodes and constant current for cylindrical electrodes. If a protocol of constant temperature is used, such as that employed in RF thermal ablation procedures in which the active electrode includes a sensor to measure temperature and the voltage is modulated to keep the temperature constant in the sensor, the tissue temperature will reach a maximum value dependent on the set target value. Under this condition, it is expected that temperature will not increase ad infinitum even with cylindrical electrodes in tissue without blood perfusion.

The novelty of this study was to assess from a formal mathematical point of view whether the geometry of the electrodes (spherical or cylindrical), the presence or absence of internal cooling, and the presence of blood perfusion, could influence the dynamic behavior of the temperature, and in particular, the conditions under which the temperature could reach a steady-state. We are aware that the real situation does not consist either of infinitely long cylindrical electrodes or spherical electrodes completely surrounded by tissue, but of needle-like electrodes based on a finitely long cylinder with a sharp tip, or electrodes with a hemispherical portion bounded by a cylindrical prism. What our results suggest is that the tissue temperature in the vicinity of the cylindrical zone will have a similar performance to the case of a cylindrical electrode, while the tissue temperature near the electrodes spherical zone will behave like a spherical electrode.

5. **Conclusions.** This study has assessed from a formal mathematical point of view whether the geometry of the electrodes (spherical or cylindrical), the presence or absence of internal cooling, and the presence of blood perfusion, could influence the dynamic behavior of the temperature, and in particular, the conditions under which the temperature could reach a steady-state. The analytical solutions have demonstrated that tissue temperature reaches a steady value in all the cases considered except for cylindrical coordinates without the blood perfusion term (both dry and cooled electrode), in which temperature increases to infinity. However, when the boundary condition is assumed to be at far, but a finite distance, the tissue temperature reaches a steady value in all cases.

REFERENCES

[1] B. L. Yun, J. M. Lee, J. H. Baek, S. H. Kim, J. Y. Lee, J. K. Han and B. I. Choi, Radiofrequency ablation for treating liver metastases from a non-colorectal origin, *Korean Journal Radiology*, **12** (2011), 579–587.

[2] E. R. Cosman Jr. and E. R. Cosman Sr., Electric and thermal field effects in tissue around radiofrequency electrodes, *Pain Medicine*, **6** (2005), 405–424.
[3] A. Thiagalingam, C. R. Campbell, A. C. Boyd, V. E. Eipper, D. L. Ross and P. Kovoor, Cooled intramural needle catheter ablation creates deeper lesions than irrigated tip catheter ablation, *Pacing and Clinical Electrophysiology*, **27** (2004), 965–970.
[4] S. I. Cho, B. Y. Chung, M. G. Cho, J. H. Baek, C. W. Park, C. H. Lee and H. O. Kim, Evaluation of the clinical efficacy of fractional radiofrequency microneedle treatament in acne scars and large facial pores, *Dermatologic survey*, (2012), 1017–1024.
[5] T. H. Everett 4th, K. W. Lee, E. E. Wilson, J. M. Guerra, P. D. Varosy and J. E. Olgin, Safety profiles and lesion size of different radiofrequency ablation technologies: A comparison of large tip, open and closed irrigation catheters, *Journal of Cardiovascular Electrophysiology*, **20** (2009), 325–335.
[6] Y. Nakasone, O. Ikeda, K. Kawanaka, K. Yokoyama and Y. Yamashita, Radiofrequency ablation in a porcine kidney model: Effect of occlusion of the arterial blood supply on ablation temperature, coagulation diameter, and histology, *Acta Radiologica*, **53** (2012), 852–856.
[7] E. J. Berjano, Theoretical modeling for radiofrequency ablation: State-of-the-art and challenges for the future, *Biomedical Engineering Online*, **18** (2006), p24.
[8] Y. Jiang, W. Chong, M. C. Diel Rambo, L. A. Bortolaia and A. C. Valdiero, Analytical solution of temperature distributions in radiofrequency ablation due to a point source of electrical current, *60 Brasilean Conference on Dynamics, Control and Their Applications, Dincon'2007*, (2007), 21–27.
[9] M. J. Rivera, M. Trujillo, V. Romero García, J. A. López Molina and E. J. Berjano, Numerical resolution of the hyperbolic heat equation using smooted mathematical functions instead of Heaviside and dirac delta distributions, *International Communications in Heat and Mass Transfer*, **46** (2013), 7–12.
[10] J. D. Wiley and J. G. Webster, Analysis and control of the current distribution under circular dispersive electrodes, *IEEE Transactions on Biomedical Engineering*, **29** (1982), 381–385.
[11] K. M. Overmyer, J. A. Pearce and D. P. de Witt, Measurements of temperature distributions at electro-surgical dispersive electrode sites, *Transactions of the ASME, Journal of Biomechanical Engineering*, **101** (1979), 66–72.
[12] W. M. Honig, The mechanism of cutting in electrosurgery, *IEEE Transactions on Biomedical Engineering*, **22** (1975), 58–62.
[13] A. Erez and A. Shitzer, Controlled destruction and temperature distributions in biological tissues subjected to monoactive electroagulation, *Journal of Biomechanical Engineering*, **102** (1980), 42–49.
[14] D. E. Haines and D. D. Watson, Tissue heating durin radiofrequency catheter ablation: A thermodynamic model and observations in isolated perfused and superfused canine right ventricular free wall, *Pacing and Clinical Electrophysiology*, **12** (1989), 962–967.
[15] D. Haemmerich, L. Chachati, A. S. Wright, D. M. Mahvi, F. T. Lee Jr. and J. G. Webster, Hepatic radiofrequency ablation with internally cooled probes: Effect of coolant temperature on lesion size, *IEEE Transactions on Biomedical Engineering*, **50** (2003), 493–500.
[16] J. A. López Molina, M. J. Rivera, M. Trujillo and E. J. Berjano, Effect of the thermal wave in radiofrequency ablation modeling: An analytical study, *Physics in Medicine and Biology*, **53** (2008), 1447–1462.
[17] J. A. López Molina, M. J. Rivera and E. J. Berjano, Analytical model based on a cylindrical geometry to study of RF ablation with needle-like internally cooled electrode, *Mathematical Problems in Engineering,* (2012), Article ID 834807, 16 pages.
[18] M. J. Rivera, J. A. López Molina, M. Trujillo and E. J. Berjano, Theoretical modeling of RF ablation with internally cooled electrodes: Comparative study of different thermal boundary conditions at the electrode-tissue interface, *Mathematical Biosciences and Engineering*, **6** (2009), 611–627.
[19] G. N. Watson, *A Treatise on the Theory of Bessel Functions*, Cambridge Mathematical Library, Cambridge University Press, Cambridge, 1995.
[20] E. J. Berjano, E. Navarro, V. Ribera, J. Gorris and J. L. Alió, Radiofrequency heating of the cornea: An engineering review of electrodes and applicators, *Open Biomedical Engineering Journal*, **11** (2007), 71–76.
[21] M. Trujillo, J. Alba and E. J. Berjano, Relationship between roll-off occurrence and spatial distribution of dehydrated tissue during RF ablation with cooled electrodes, *International Journal of Hyperthermia*, **28** (2012), 62–68.

[22] I. A. Chang, Finite elements analysis of hepatic radiofrequency ablation probes using temperature-dependent electrical conductivity, *Biomedical Engineering Online*, **8** (2003), p12.
[23] I. A. Chang and U. D. Nguyen, Thermal modeling of lesions growth with radiofrequency ablation devices, *Biomedical Engineering Online*, **6** (2004), p27.

Received March 30, 2015; Accepted July 21, 2015.

E-mail address: jalopez@mat.upv.es
E-mail address: mjrivera@mat.upv.es
E-mail address: eberjano@eln.upv.es